P6.18   THE IMPACTS OF THUNDERSTORM GEOMETRY AND WSR-88D BEAM CHARACTERISTICS
ON DIAGNOSING SUPERCELL TORNADOES

Steven F. Piltz*
National Weather Service, Tulsa, Oklahoma

Donald W. Burgess
Cooperative Institute for Mesoscale Meteorological Studies
University of Oklahoma, Norman, Oklahoma

1.0 INTRODUCTION

Under certain circumstances data artifacts relating to storm cell geometry and WSR-88D beam characteristics can occur and appear very similar to storm-scale circulation signatures. An investigation of the tornadic and non-tornadic phases of select supercell thunderstorms suggests that these signatures can be of sufficient magnitude and possess enough spatial and temporal continuity to suggest a significant probability of tornadogenesis.

By quantifying an aspect of the WSR-88D's beam, and investigating the geometry of both the supercell and radar beam, it may be possible to more properly diagnose velocity couplets seen in storm-relative Doppler velocity data, and apply this understanding to an operational setting.

2.0 WSR-88D BEAM CHARACTERISTICS AND SIDE-LOBE CONTAMINATION

The characteristics of the WSR-88D beam pattern are predicted from parameters of the parabolic reflector and other parts of the antenna system. However, beam pattern measurements have only been made a few times. Full antenna data measurements are available only from testing by the antenna manufacturer (Andrew Corporation of Canada), testing associated with government acceptance of the radars, and from testing by NSSL on the NEXRAD research radar (KOUN) during development of Dual-Polarization (NEXRAD Program internal documents).   Figure 1 is a representative example of the antenna test data. As a result of the lack of measured data, discussions of WSR-88D beam characteristics rely on assumptions that all antennas and beam patterns at least generally conform to the test data and predicted characteristics.

The curved data plot (Fig. 1) is the actual measurement, while the solid straight lines depict the antenna design specifications. In particular, it is

---

* Corresponding Author Address: Steven Piltz, National Weather Service, Tulsa, OK 74128-0320; e-mail: steven.piltz@noaa.gov
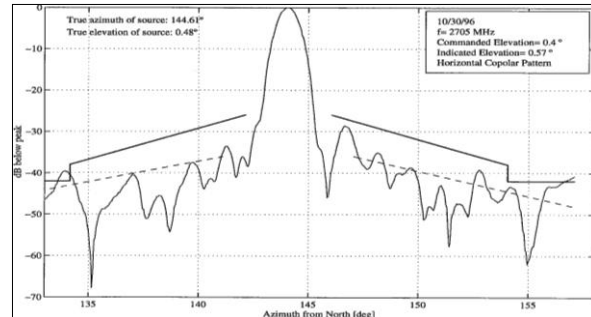
Figure 1 - Antenna radiation pattern for KOUN WSR-88D as measured by NSSL (NEXRAD Program, 2008). Curved line is actual measurement and solid/dashed linear lines depict antenna design specifications.

assumed for WSR-88D radars that: 1) the half power (3 dB below peak gain) points define a beam width of just
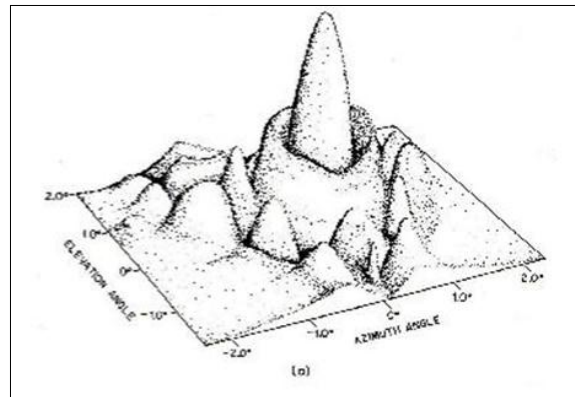

Figure 2 - Typical three-dimensional Cartesian plot of complete beam pattern. From Skolnick (1990).

less than 1 degree (0.9 deg to 1.0 deg depending on exact frequency), 2) the first side-lobes peaks are 27 dB or more below the main peak and are located 2.5 deg. to 3.0 deg. from the azimuth of beam center, 3) received power in a side-lobe is 54 dB (twice 27 dB) or more below the power in the main lobe because the antenna is used for illumination and for energy return; this is the so-called 2-way side-lobe, and 4) second and higher order side-lobes have 10 dB or less power than the first side-lobes and can be ignored in practical application (NEXRAD Program, 2008).

Although all testing and first thought about antenna side-lobes concern horizontal measurements, the antenna pattern is to first approximation circular, and antenna side-lobes are 3-dimensional. As seen in Figure 2, the prominent first side-lobe extends all around the main lobe. Thus, when thinking of side-lobe contamination of data assumed to come from the main lobe, one must consider vertical as well as horizontal contributions.

Warning forecasters need to take side-lobes into consideration when analyzing WSR-88D data and diagnosing the importance of velocity signatures. Velocity data that appear to be from the main beam location may actually be from or contaminated by side-lobe return from ~3 degrees in azimuth on either side of the center of the main beam and/or ~3 degrees above the center of the main beam. As a rule of thumb for an individual radar gate, if power returns from two sources (main beam and side-lobe in this case) are within 5 dB or less of each another, then contamination of the velocity estimate for that gate is increasingly likely. For example, if the reflectivity in the side-lobe is 59 dBZ and the reflectivity in the main beam is 10 dBZ (within 5 dB of the 54 dB difference between side-lobe and main-beam powers), contamination of the mean velocity estimate at that location must be considered. Sharp gradients in mean velocities with broad spectral widths in potential side-lobe contribution locations should be viewed with suspicion, and a check should be made for possible contamination from horizontal or vertical side-lobes.

3.0 A SIDE-LOBE CONTAMINATION CASE

The focus of this investigation is the vicinity of the updraft region of supercell thunderstorms where high radar reflectivity values aloft can exist above low values near the surface. Typically referred to as the "over-hang", this vertical reflectivity gradient is strong enough in some supercells to exceed the predicted threshold
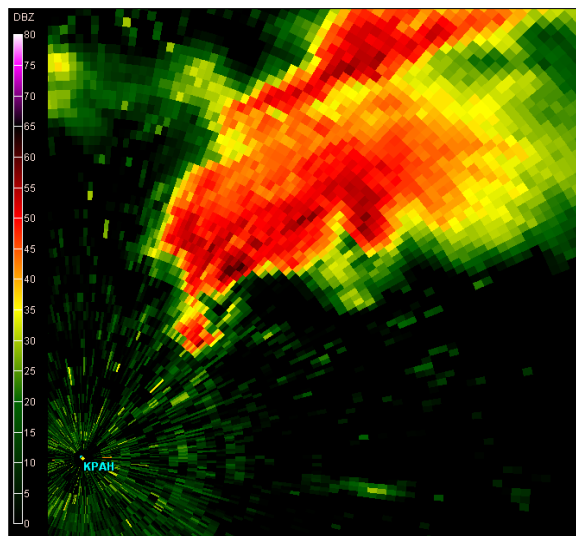
Figure 3 – KPAH reflectivity from the 0.5 degree elevation scan at 2055 UTC 22 September, 2006.

thought necessary to result in side-lobe contamination. Data from the KPAH (Paducah, KY) WSR-88D on 22 September, 2006 illustrate this.

Reflectivity data from the 0.5 degree elevation slice (Fig. 3) of the KPAH radar at 2055 UTC 22 September, 2006 show a thunderstorm immediately northeast of the radar. The storm is a supercell and
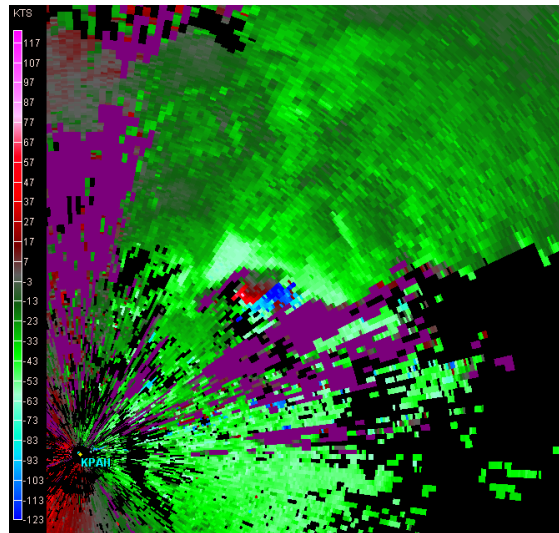
Figure 4 – KPAH storm-relative velocity from the 0.5 degree elevation scan at 2055 UTC 22 September, 2006. Storm motion is from 245 degrees at 18 m/s.
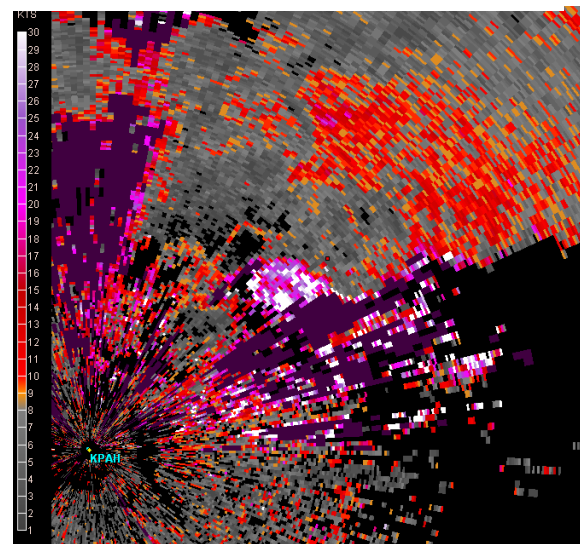
Figure 5 – KPAH spectrum width from the 0.5 degree elevation scan at 2055 UTC 22 September, 2006

moved approximately from 245 degrees at 18 m/s. High values of inbound and outbound storm-relative velocity data (Fig. 4) are seen in close proximity in the southern portion of the storm. The extreme and chaotic appearance

of these data suggest quality issues, including likely dealiasing failures. Very high values of the spectral component (Fig. 5) further imply data reliability problems.

A cross-section (Fig. 6) through the collocated low-reflectivity area and suspect velocity data reveals values of -3 dBZ near the ground, and values as high as 60
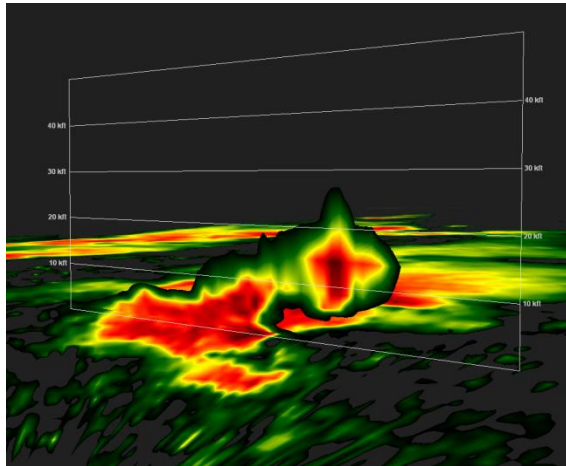

Figure 6 – Reflectivity cross-section of KPAH data from 2055 UTC 22 September, 2006

dBZ in the reflectivity over-hang. Given we are comparing reflectivities in the vertical and nearly vertical, the range normalization performed in
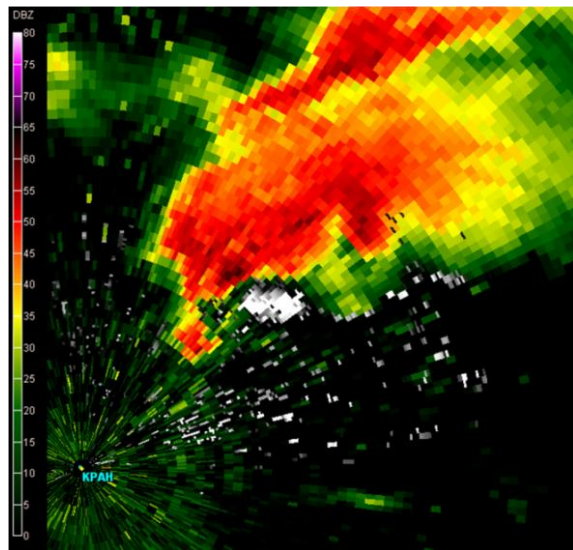

Figure 7 - KPAH reflectivity from the 0.5 degree elevation scan at 2055 UTC 22 September, 2006, with the corresponding suspect velocity data collocated in grayscale.

calculating reflectivity in dBZ is negligible. Therefore reflectivity expressed in dBZ, as routinely seen operationally by forecasters, can be used to evaluate

the predicted beam characteristics expressed in dB. The reflectivity gradient in this cross-section well exceeds the 49 dB value that is estimated to be the threshold where side-lobe contamination is expected to become increasingly likely. Thus, it is very likely that strong outbound velocities in the high reflectivity region aloft (not shown) have been mis-mapped to the 0.5 degree elevation slice everywhere the difference in returned power from a side-lobe signal and energy from the center of the beam exceeded a threshold.

To test if the weak reflectivity in the 0.5 degree data correlated with the suspect data, as it should if side-lobe contamination were occurring, the suspect velocity pixels from Figure 4 were converted back to base velocities and mapped in grayscale onto the reflectivity (Fig. 7). Because these velocity data fit into the reflectivity pattern with some precision, it is logical to conclude that the weak reflectivity and vertical reflectivity profile were contaminating the 0.5 degree velocity data. (The lower the 0.5 degree reflectivity, the more readily a vertical reflectivity gradient sufficient to allow side-lobe contamination can occur.)

The unusual character of these velocity data in the 2055 UTC volume scan is such that questioning its quality would not be unexpected. Those data from two volume scans later at 2011 UTC (Fig. 8) are more problematic, and show two cyclonic velocity couplets associated with the supercell.

A cross-section (not shown) through the couplet closest to the KPAH radar, along with a plan view reflectivity plot, reveals that this couplet was contained within a classic hook echo. A tornado was occurring at this time with this mesocyclone.
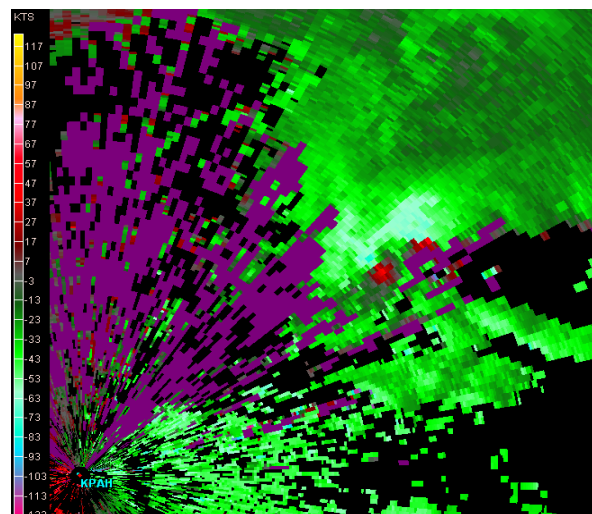

Figure 8 – KPAH storm-relative velocities from the 0.5 degree elevation scan at 2111 UTC 22 September, 2006. Storm motion is from 245 degrees at 18 m/s.

A reflectivity cross-section through the couplet furthest from the KPAH radar (Fig. 9) indicates the velocity data of interest are within the low reflectivity area in the 0.5 degree elevation scan and beneath reflectivity values as high as 58.5 dBZ. Based on this cross-section, it is
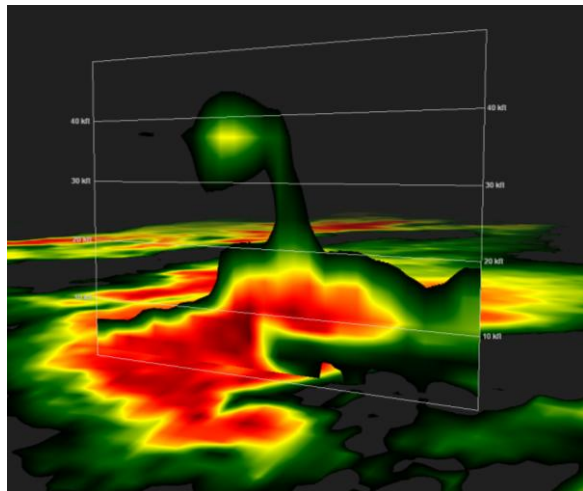

Figure 9 – Reflectivity cross-section of KPAH data from 2111 UTC 22 September, 2006.

likely that side-lobe contamination occurred, and the conclusion is drawn that high velocity outbound data aloft contaminated the velocity data from the 0.5 degree elevation. The contamination caused high outbound velocities to be juxtaposed with the higher inbound velocity values. The result is a velocity pattern that at least to some degree mimics that which would be expected to be associated with a mesocyclone.
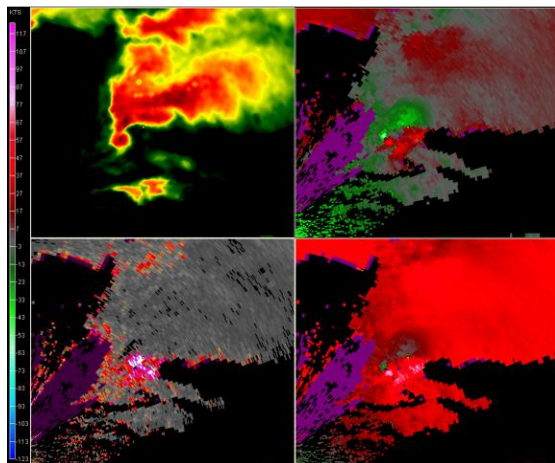

Figure 10 – KPAH data at 2111 UTC. All data from the 1.4 degree elevation scan.   Reflectivity upper-left, spectrum width lower-left, storm-relative velocity upper-right, base velocity lower-right.

Because this particular thunderstorm is of sufficient depth, and is in close proximity to the radar, both the signature associated with the tornadic mesocyclone (closest to the radar), and that which appears to be a

radar artifact, can be seen in data from the 1.4 degree elevation scan (Fig. 10) at 2111 UTC, giving a degree of height continuity to the suspect signature. Note the high spectrum width values associated with the suspect velocity couplet.
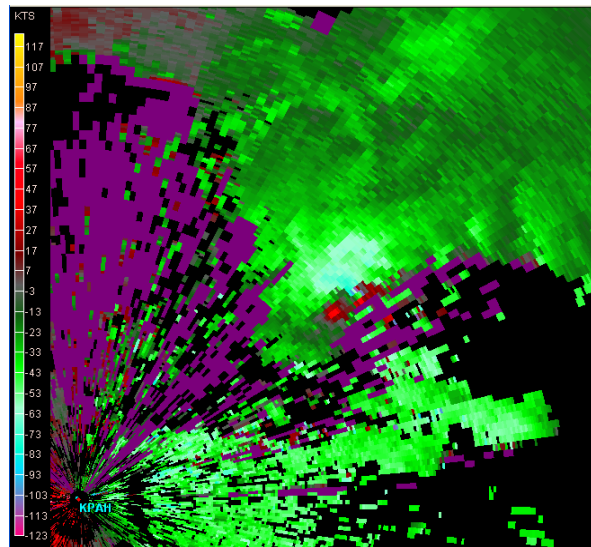

Figure 11 – KPAH storm-relative velocity from the 0.5 degree elevation scan at 2106 UTC 22 September, 2006. Storm motion is from 245 degrees at 18 m/s.

Data from volume scans at 2106 UTC (Fig.11) and 2111 UTC (Fig. 8) provide examples of how both the couplet associated with the tornadic mesocyclone and the suspect couplet translate coherently with time. As long as the geometry of the radar beam and the storm remain in a quasi-stationary relationship, the suspect data signatures would be expected to track with the cell, providing temporal continuity to the signatures.

4.0 DISCUSSION AND FUTURE WORK

Because of the limited amount of specific information available on the beam characteristics of the National Weather Service's WSR-88Ds, the occurrence of side-lobe contamination can only be reasoned from the data, and not explicitly flagged.   To conclude side-lobe contamination in this case, predicted beam characteristics were used in conjunction with spectrum width values, echo geometry, and a review of the National Weather Service's Storm Data file that had only a single tornado logged during the time period that the authors examined data from the thunderstorm.

When, as in this case, those velocity data that are considered suspect also resemble signatures that may prompt a public severe weather warning, the challenge to understand those data take on a great importance. Further, this case brings into focus that one of the most likely locations for reoccurring side-lobe contamination is the inflow region of a supercell thunderstorm.

The authors have also noted rotational velocity signatures in other cases that offer similar challenges that cannot be explained solely by side-lobe contamination using the predicted threshold. One of several possible explanations for these cases is near zero Doppler velocities in erect updrafts. When fast storm motions are subtracted from these low base velocities, the result is a perceived strong storm-relative velocity. Data from the Peachtree, GA WSR-88D (KFFC) on 02 February, 2009 are used to describe this possibility.

At 0008 UTC on 02 February, 2009, the KFFC radar retrieved data from a supercell thunderstorm to its southeast. The white marker in both images in Figure 13 are in the same geographic location. The marker is centered over the strong gate-to-gate couplet in those storm-relative velocity data. While it is plausible that the rotational signature marks a vorticity center in the east hemisphere of the mesocyclone, it is also possible that it is the result of subtracting the storm's motion from low base velocities (Fig. 14) in the updraft. While it is understood that the shear across a velocity signature is independent of the storm motion, interpretation of that shear assumes a quasi-horizontal flow in the signature, and not a transition to vertical flow as is occurring in the inflow region of a supercell. Further work to understand such concepts continues. Data from VORTEX II may ultimately provide some understanding.
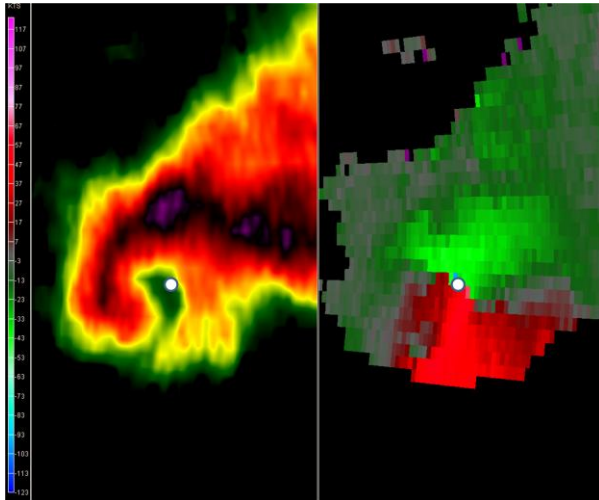

Figure 13 – KFFC data at 0008 UTC 02 February, 2009. Data from the 0.5 degree elevation scan. Reflectivity left, storm-relative velocity right. Storm motion is from 270 degrees at 21 m/s. The white markers are located in the same geographic location.

While not formally studied, the authors are aware that National Weather Service Tornado Warnings have been issued in situations similar to those discussed in this work. Anecdotal evidence suggests that the percentage of such warnings may be large enough to impact the agency's tornado warning false alarm scores. Further, there are obvious implications to path-casts that

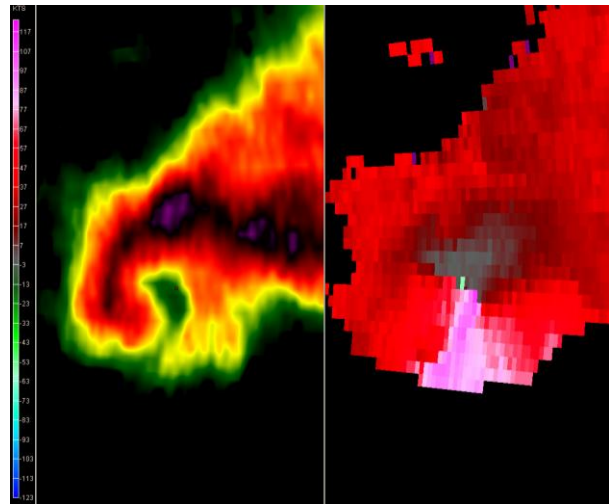are sometimes used in National Weather Service warnings and statements.

Figure 14 – As in Figure 13, except base velocity is shown to the right.

The authors believe that work is needed to better quantify the beam of all WSR-88Ds in hopes of more definitively determining side-lobe contamination issues, and to develop techniques for the operational assessment of side-lobe contamination.

5.0 REFERENCES

NEXRAD Program, 2008: Informal, unpublished documents available from the second author upon request

Skolnick, M.I., 1990: /Introduction to Radar Systems/, New York, NY, McGraw-Hill Book Co., 581 pp.